Lindsay E. Wu,[1,2] Christopher C. Meoli,[1] Salvatore P. Mangiafico,[3] Daniel J. Fazakerley,[1] Victoria C. Cogger,[4] Mashani Mohamad,[4,5] Himani Pant,[1] Myung-Jin Kang,[2] Elizabeth Powter,[6] James G. Burchfield,[1] Chrysovalantou E. Xirouchaki,[3] A. Stefanie Mikolaizak,[7] Jacqueline Stöckli,[1] Ganesh Kolumam,[8] Nicholas van Bruggen,[8] Jennifer R. Gamble,[6] David G. Le Couteur,[4] Gregory J. Cooney,[1] Sofianos Andrikopoulos,[3] and David E. James[1,9]

Systemic VEGF-A Neutralization Ameliorates Diet-Induced Metabolic Dysfunction

Diabetes 2014;63:2656–2667 | DOI: 10.2337/db13-1665

The vascular endothelial growth factor (VEGF) family of cytokines are important regulators of angiogenesis that have emerged as important targets for the treatment of obesity. While serum VEGF levels rise during obesity, recent studies using genetic models provide conflicting evidence as to whether VEGF prevents or accelerates metabolic dysfunction during obesity. In the current study, we sought to identify the effects of VEGF-A neutralization on parameters of glucose metabolism and insulin action in a dietary mouse model of obesity. Within only 72 h of administration of the VEGF-A–neutralizing monoclonal antibody B.20-4.1, we observed almost complete reversal of high-fat diet–induced insulin resistance principally due to improved insulin sensitivity in the liver and in adipose tissue. These effects were independent of changes in whole-body adiposity or insulin signaling. These findings show an important and unexpected role for VEGF in liver insulin resistance, opening up a potentially novel therapeutic avenue for obesity-related metabolic disease.

Vascular endothelial growth factor (VEGF) proteins are a subgroup of the platelet-derived growth factor family and comprise four members, including VEGF-A, VEGF-B, VEGF-C, and VEGF-D, which bind their cognate receptors Flt-1 and Flk-1 to promote angiogenesis (1). Though classically studied in the context of angiogenesis stimulation in endothelial cells, VEGF receptors are present in a wide range of cell types and exhibit pleiotropic effects outside of angiogenesis (2,3). For example, VEGF-B was recently shown to regulate lipid transport across endothelial cells (4). This is mediated by transcriptional induction of fatty acid transporters, leading to enhanced transendothelial transport of fatty acids and promoting their delivery to tissues such as heart and muscle. Deletion of VEGF-B reduces ectopic lipid deposition and improves insulin sensitivity in dietary and genetic models of obesity in mice (5), and this evidence has been used to suggest a role for VEGF-B in type 2 diabetes and the metabolic syndrome.

The role of VEGF and angiogenesis in obesity and diabetes has become somewhat confused due to a number of recent conflicting studies (6–8). Serum levels of VEGF-A are raised during obesity (9–11) and rapidly decrease

[1]Diabetes and Obesity Program, Garvan Institute of Medical Research, Darlinghurst, New South Wales, Australia
[2]Laboratory for Ageing Research, School of Medical Sciences, UNSW Australia, New South Wales, Australia
[3]Department of Medicine (Austin Health), The University of Melbourne, Heidelberg, Victoria, Australia
[4]Centre for Education and Research on Ageing and ANZAC Medical Research Institute, University of Sydney and Concord Hospital, Concord, New South Wales, Australia
[5]Faculty of Pharmacy, Universiti Teknologi MARA, Bandar Puncak Alam, Selangor, Malaysia
[6]Centre for the Endothelium, Vascular Biology Program, Centenary Institute, and The University of Sydney, Sydney, Australia
[7]Falls and Balance Research Group, Neuroscience Research Australia, Sydney, Australia
[8]Department of Biomedical Imaging, Genentech Inc., San Francisco, CA
[9]Charles Perkins Centre, School of Molecular Bioscience, The University of Sydney, Sydney, Australia

Corresponding author: David E. James, david.james@sydney.edu.au.

Received 28 October 2013 and accepted 27 March 2014.

This article contains Supplementary Data online at http://diabetes.diabetesjournals.org/lookup/suppl/doi:10.2337/db13-1665/-/DC1.

L.E.W. and C.C.M. contributed equally to this work.

© 2014 by the American Diabetes Association. Readers may use this article as long as the work is properly cited, the use is educational and not for profit, and the work is not altered.

following bariatric surgery (10), suggesting that elevated VEGF is deleterious. In support of this Lu et al. (12) showed that VEGF knockdown suppressed obesity and promoted "browning" of white adipose tissue (WAT). In contrast, reports using adipose-specific VEGF transgenic or knockout mice suggest that increased expression of VEGF is beneficial during obesity (12–15). This is further complicated by contradictory reports depending on the model system; Sun et al. (13) found that antibody neutralization of VEGF impaired metabolic homeostasis in a dietary model of obesity but improved glucose tolerance in a genetic (*ob/ob*) model. These inconsistencies may be due to the following reasons. In two of these studies (14,15), the *Fabp4* promoter was used to achieve adipose-specific overexpression or deletion using the Cre-LoxP system. This promoter is not specific to adipose tissue (16), meaning that the observed effects may be the result of VEGF-A changes in nonadipose tissues. In particular, FABP4 is expressed in microvascular endothelial cells (17), which are a key target of VEGF and present in tissues throughout the body. Secondly, in addition to its role as an extracellular signaling factor, VEGF displays intracellular, cell-autonomous regulation of cell signaling (18,19). It may be that the effects observed with genetic VEGF overexpression or deletion may reflect changes in intracellular signaling rather than changes in extracellular VEGF signaling, which is selectively targeted by neutralizing antibodies. Lastly, the possibility remains that adipose tissue may not be the most important site of action for VEGF in mediating changes in insulin sensitivity. This would be consistent with studies reporting that systemic administration of antiangiogenic compounds improves insulin sensitivity (20–22).

To address the issues described above, we determined the temporal relationship between changes in whole-body adiposity and glucose homeostasis upon blockade of extracellular VEGF signaling in mice following administration of a VEGF-A–neutralizing antibody (23). We show that systemic VEGF-A neutralization is an effective and rapid strategy for preventing as well as reversing diet-induced insulin resistance in short- and long-term models of high-fat feeding. These effects occur within a short timeframe (72 h), involving almost complete amelioration of impaired hepatic insulin sensitivity and occur independently of adiposity (20–22,24,25) and insulin signaling.

RESEARCH DESIGN AND METHODS

Mice

Male C57BL6 mice were from Australian BioResources (Moss Vale, New South Wales, Australia). Animals were obtained at 7 weeks of age and acclimatized for 1 week prior to experiments. Mice were maintained on a 12 h light/dark cycle (0700/1900 h) at a temperature of 22 ± 1°C with 80% relative humidity and provided ad libitum access to food and water. Experiments were carried out in accordance with guidelines for animal research from the National Health and Medical Research Council (NHMRC; Australia) and were approved by Garvan Institute animal ethics committee.

Diets

Diets were as previously described (26,27). Chow diet (Gordon's Specialty Stock Feeds, Yanderra, New South Wales, Australia) comprised 8% calories from fat, 21% calories from protein, and 71% calories from carbohydrate, with total energy density of 2.6 kcal/g. High-fat diet (HFD) was 45% calories from fat (beef lard), 20% calories from protein, and 35% calories from carbohydrate at a density of 4.7 kcal/g, based on rodent diet D12451 (Research Diets, New Brunswick, NJ).

VEGF Neutralization

VEGF-A was neutralized using the antibody B20-4.1 (23) from Genentech. Control antibody was mouse IgG (Sigma-Aldrich). Antibodies were diluted in physiological saline and administered by intraperitoneal injection at 5 mg/kg body weight.

Western Blots

WAT samples were from 6-h–fasted or acute insulin–stimulated (5 units/kg, 10 min) mice maintained on chow of HFD for 3 days with VEGF or control IgG injection. Liver samples were snap frozen following hyperinsulinemic–euglycemic clamps. Densitometry was performed using Odyssey software (LI-COR Inc.). n = 3–5 mice per group. Antibodies used for Western blots were from Santa Cruz Biotechnology, CA (14-3-3, sc-629); Cell Signaling Technologies, MA (phospho-S6K, 9205; phospho-S473 Akt, 4051; phospho-T308 Akt, 9275; total Akt, 9272; phospho–hormone-sensitive lipase [HSL]; total HSL); and Vala Sciences (phospho-perilipin).

Glucose and Insulin Tolerance Tests

Glucose challenge was as previously described (27–29). Mice were fasted for 6 h beginning at 0800 h. Glucose was administered by intraperitoneal injection using a 25% glucose solution to achieve a final dose of 1 g/kg, and blood glucose was measured with an Accu-Chek Performa (Roche). Total area under the curve (AUC) was calculated using the trapezoidal formula. Blood samples were obtained via tail bleeds using 5 μL heparinized hematocrit tubes (Drummond) and ejecting samples into a mouse ultrasensitive insulin ELISA (90080, Crystal Chem). Insulin tolerance test protocol was identical to glucose tolerance test (GTT), using 0.75 units/kg insulin diluted in saline.

Tracer Uptake

^{3}H-2-deoxyglucose (2-DOG; 2 μCi/25 g body weight) was coinjected with glucose during the GTT as above. Blood samples were obtained at 15, 30, 60, and 120 min using 5 μL heparinized hematocrit tubes (Drummond) and immediately added to 100 μL saturated BaOH solution. At 120 min, mice were culled and tissues were snap frozen. Protein was precipitated from blood with saturated $ZnSO_4$ solution, and radioactivity was measured in supernatants. Frozen tissues were powdered, weighed, and homogenized in 500 μL H_2O, and soluble supernatant was collected. Supernatant (150 μL) was diluted to 1 mL and added to

4 mL scintillation fluid (Ultima Gold, PerkinElmer) for total counts. To determine free (nonphosphorylated) glucose counts, anion exchange columns were prepared using AG 1-X8 resin (Bio-Rad) washed extensively in dH_2O. Supernatant (150 μL) was applied to anion exchange columns and eluted with three 1 mL dH_2O wash steps. Of this combined elution, 1 mL was diluted into 4 mL scintillation fluid. Vortexed samples were read on a Beckman LS 6500 β-counter. 2-Deoxyglucose uptake and phosphorylation in tissues was determined by subtracting AG 1-X8 resin eluate readings from total, homogenized tissue readings and normalized for tissue weight, blood glucose concentrations during the GTT, and radioactive AUC determined from blood samples taken during the GTT.

Hyperinsulinemic Clamps

Hyperinsulinemic–euglycemic clamps were performed in 5-h–fasted mice as previously described (30). In the current study, an initial priming dose of insulin was followed by constant infusion at a rate of 10 mU/kg/min. Euglycemia was maintained by variable infusion of 2.5–10% glucose solution. Glucose turnover was calculated using Steele steady-state equation.

Adipocyte Diameter Measurements

Whole tissue sections were imaged on a Leica DM6000 Power Mosaic. Adipocyte area was analyzed in a blind, semiautomated fashion using custom macros written in ImageJ.

Endothelial Cell Proliferation

Human umbilical vein endothelial cells were plated at 4×10^3 cells per well in 96-well culture plates, and 10 ng/mL VEGF-A or VEGF-B (R&D Systems) was preincubated with 1.5 μg/mL anti-VEGF-A antibody for 15 min then added to cells. Cell number was assessed with the MTS (3-[4,5-dimethylthiazol-2-yl]-5-[3-carboxymethoxyphenyl]-2-[4-sultophenyl]-2H-tetrazolium) assay (Promega) on days 0 and 3.

Quantitative PCR

RNA was extracted using Tri reagent (Sigma-Aldrich). cDNA synthesis (DyNAmo kit, Thermo Scientific) was performed with 1 μg RNA. Gene expression of four housekeeper genes (*tbp*, *ywhaz*, *b2m*, and *hprt*) was measured, and the geometric means of the two most stable housekeepers, determined using NormFinder, were used to normalize expression of *Flt-1* (VEGF receptor Flt-1) and *Kdr* (VEGF receptor Flk-1). Samples were run in technical triplicate on a Roche LightCycler 480 using LightCycler 480 SYBR I Green Master Mix. qPCR primers used were *Flt1* (F: TTGTAAACGTGAAACCTCAG; R: GATTCT TCATTCTCAGTGCAG), *Kdr* (F: AATGGTACAGAAATGGA AGG; R: GCATCTCTTTCAGTCACTTC), *B2m* (F: GTATGCT ATCCAGAAAACCC; R: CTGAAGGACATATCTGACATC), *Hprt* (F: AGGGATTTGAATCACGTTTG; R: TTTACTGGCA ACATCAACAG), *Tbp* (F: GTTCTTAGACTTCAAGATCCAG; R: TTCTGGGTTTGATCATTCTG), and *Ywhaz* (F: ACTTAA CATTGTGGACATCG; R: GGATGACAAATGGTCTACTG).

Triglyceride and Glycerol Measurements

Lipids were extracted using Folsch reagent, and triglyceride content was measured using an assay kit (Roche/Hitachi 11730711 216 triglycerides GPO-PAP) according to manufacturer's instructions. Glycerol was assayed in plasma using a free glycerol determination kit (Sigma-FG0100) as per manufacturer's instructions.

Serum Cytokine and Metabolic Hormone Analysis

Serum cytokines are measured using Luminex multiplex assay (Bio-Rad Mouse Grp I 23-plex), and serum metabolic hormones were measured using Milliplex Mouse Metabolic 14-plex kit (Millipore) Luminex assay.

Scanning Electron Microscopy

Hepatic sinusoidal fenestrations were measured in perfused livers by scanning electron microscopy as recently described (31).

Statistics

Independent one-way ANOVA was used to compare scores of normally distributed continuous variables. Post hoc analysis was conducted to determine significant difference between groups. Type 1 errors were controlled for by applying a Bonferroni adjustment. One-way between-group ANOVA was tested using the Kruskal–Wallis test where data were not normally distributed. GTT data are shown as median values, error bars represent interquartile range. For GTTs, total AUCs were used for analysis. Box plots are shown in Tukey plot format. All analysis was performed using SPSS.

RESULTS

To investigate the role of VEGF-A on metabolic activity in vivo, we used the selective VEGF-A neutralizing antibody B20-4.1, which has previously been characterized on an in vitro, in vivo, and structural basis (23,32). To further test the specificity of B20-4.1, we measured the ability of this antibody to suppress the biological activity of either mouse VEGF-A or VEGF-B in primary endothelial cells. Consistent with previous findings, B20-4.1–suppressed VEGF-A, but not VEGF-B, stimulated endothelial cell proliferation (Fig. 1).

VEGF-A Neutralization Blocks the Onset of Diet-Induced Glucose Intolerance

To investigate the role of VEGF-A in metabolic dysfunction, 8-week-old C57BL6 males were randomly assigned to treatment groups, and an initial baseline GTT was performed (Fig. 2*A* and *B*). Mice were then given a single intraperitoneal injection with either the VEGF-A–neutralizing antibody B20-4.1 or the control antibody (5 mg/kg body weight) and immediately placed on either chow diet or HFD. The VEGF-A–neutralizing antibody raised circulating VEGF-A levels, consistent with decreased clearance of antibody-bound VEGF-A as described previously (Supplementary Fig. 1) (1,33–35), and surprisingly, a trend toward decreased VEGF receptor expression was observed (Supplementary Fig. 1*B* and *C*). Three days of high-fat feeding

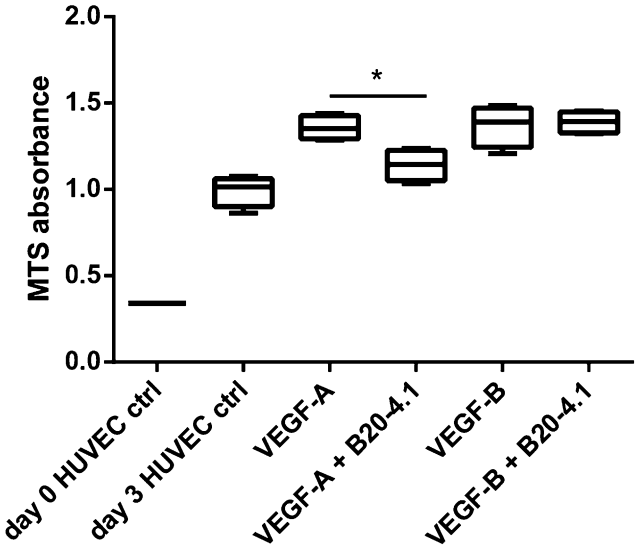

Figure 1—Biological activity of VEGF-A–neutralizing antibody B20-4.1. Human umbilical vein endothelial cells were incubated as indicated with either recombinant mouse VEGF-A or VEGF-B (10 ng/mL) in the presence or absence of the VEGF-A–neutralizing antibody B20-4.1 (1.5 μg/mL). *$P < 0.05$, Mann–Whitney test. ctrl, control; HUVEC, human umbilical vein endothelial cell.

was sufficient to cause a pronounced decrease in whole-body glucose tolerance, with increased fasting glucose levels (Table 1). Treatment with the VEGF-A antibody almost completely prevented the impaired glucose tolerance observed in HFD animals (Fig. 2*C* and *D*). These changes occurred without any significant change in circulating insulin levels in either the basal or glucose-stimulated state (Table 1, Fig. 2*E*). To determine which tissues were contributing to these changes, we next administered ^{3}H-2-DOG during the GTT and measured uptake into skeletal muscle and WAT (Fig. 2*F* and *G*). As evidence of improved insulin action, we observed increased 2-DOG uptake into WAT, but not quadriceps, in mice treated with the VEGF-A during high-fat feeding.

VEGF-A Neutralization Reverses Glucose Intolerance During Long-term High-Fat Feeding

In addition to acute studies, we next wanted to determine if VEGF-A neutralization could reverse insulin resistance in long-term high-fat–fed mice. Male (8 weeks old) C57BL6 mice were placed on HFD for 4 weeks to establish obesity, glucose intolerance, and insulin resistance. This was sufficient to trigger more profound glucose intolerance than observed after 3 days of high-fat feeding concomitant with a significant increase in fasting hyperglycemia (Fig. 3). Similar to our previous studies (Fig. 2*B*), only two injections of VEGF-A–neutralizing antibody were sufficient to improve glucose tolerance in high-fat fed animals (Fig. 3*B*), and this improvement was sustained for at least 17 days after the last dose of antibody (Fig. 3*B*–*E*). One observation was the substantial reduction in fasting blood glucose following treatment with the VEGF antibody (Supplementary Fig. 2). Insulin tolerance was also assessed as a direct measure of insulin sensitivity (Fig. 4). The glucose-lowering effect of insulin in the VEGF-neutralized mice appeared limited by the significantly lower fasting glucose levels in these mice, complicating interpretation of these data. By 21 days post injection, the ameliorating effects of the VEGF-A–neutralizing antibody on glucose tolerance were no longer evident (Fig. 3*F*). The eventual loss of an effect on glucose tolerance may reflect a decline in the downstream effects of VEGF-A neutralization or alternatively the eventual clearance of the neutralizing antibody. These data suggest that VEGF-A inhibition is an effective and persistent strategy for treating preexisting metabolic dysfunction. Moreover, in view of the reversibility of the effects on metabolism, this suggests that the VEGF antibody is targeting a regulatory parameter that is highly plastic. After this 21-day period, mice were maintained on their respective diets without further intervention for an additional 3 weeks (Fig. 3*A*). Mice were again treated with a single dose of VEGF-A or control antibody (5 mg/kg body weight) and subjected to a GTT 72 h later (Supplementary Fig. 3). Again, this single retreatment with the VEGF-A–neutralizing antibody rapidly reinitiated a significant improvement in whole-body glucose tolerance in long-term high-fat–fed animals. This provides significant evidence in favor of the therapeutic potential of this reagent for the treatment of metabolic disease.

VEGF-A Neutralization Improves Hepatic Insulin Sensitivity

Whole-body insulin action in mammals is largely governed by insulin action in muscle and liver. Our analysis of ^{3}H-2-DOG uptake during the GTT revealed no significant effect of VEGF neutralization in muscle and a significant improvement in WAT. During acute high-fat feeding, whole-body insulin resistance is largely due to impaired insulin action in the liver (36), which precedes insulin resistance in muscle (37). This is consistent with our observation of no change in 2-DOG uptake into muscle or fat with high-fat feeding, despite profound glucose intolerance (Fig. 2). To investigate this, we used the hyperinsulinemic–euglycemic clamp method (Fig. 5). After 3 days of high-fat feeding, the whole-body glucose infusion rate in response to a 10 mU/kg/min insulin infusion was reduced by >80% compared with the chow-fed group. This inhibitory effect was almost completely abolished by one single dose of the VEGF-neutralizing antibody prior to commencement of the HFD (Fig. 5*A*). There was a tendency toward increased peripheral glucose disappearance in VEGF-treated animals, but this failed to reach statistical significance ($P = 0.08$) (Fig. 5*B*). More strikingly, VEGF neutralization completely prevented HFD-induced hepatic insulin resistance as indicated by measurement of endogenous glucose production (Fig. 5*C*). These data are in agreement with previous studies also showing that insulin resistance during short-term high-fat feeding is mediated by decreased suppression of hepatic glucose output, rather than peripheral insulin resistance (36), and suggest

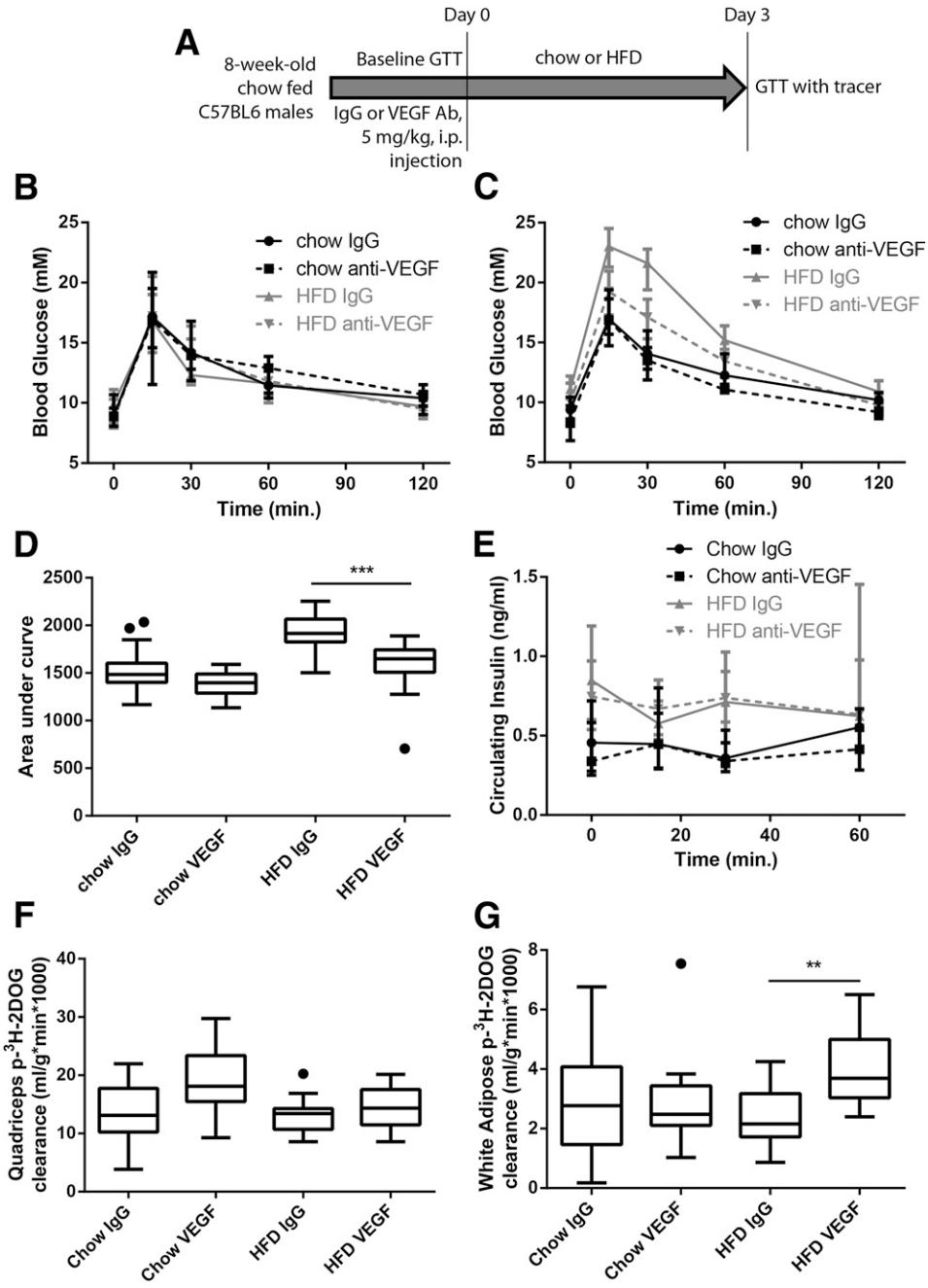

Figure 2—Glucose tolerance during VEGF neutralization in acute high-fat fed mice. *A*: Schema for experiment. *B*: Chow-fed mice were randomly assigned to treatment groups and baseline glucose tolerance was measured. Immediately following baseline GTT, mice were injected (5 mg/kg, intraperitoneally) with either VEGF-neutralizing or control (IgG) antibody and placed on chow diet or HFD. *C*: Three days after injection and diet, glucose tolerance was again assessed and quantified by (*D*) total AUC. *E*: Blood insulin levels were measured during GTT. Phosphorylated ^{3}H-2-DOG uptake into (*F*) quadriceps and (*G*) epididymal WAT during GTT was assessed to determine rates of glucose uptake. *B* and *C*: n = 22–27 mice per treatment across four independent cohorts. *E*–*G*: n = 14–19 mice per treatment across three independent cohorts. ***$P < 0.001$; **$P < 0.01$, Kruskal–Wallis test. Glucose and insulin levels are plotted as median values, and error bars are interquartile range. Large dots are outliers, as per representation of data using Tukey box plot format.

that VEGF neutralization prevents HFD-induced insulin resistance largely through changes in the liver.

In an effort to further explore the mechanism of VEGF neutralization on hepatic and WAT insulin action, we next examined insulin signaling. We did not observe any significant difference in insulin-stimulated Akt signaling with VEGF neutralization (Supplementary Fig. 4). We then sought to determine whether changes in circulating cytokines could account for these effects and measured a panel of cytokines in the serum of VEGF- or control IgG-treated

Table 1—Effects of VEGF-neutralizing antibody on metabolic parameters in chow- and high-fat–fed mice during an acute model of high-fat feeding

Parameter	Chow IgG	Chow anti-VEGF	HFD IgG	HFD anti-VEGF
Fasting glucose, mmol/L	9.4 (8.4–10.5)	8.6 (8.2–9.7)	10.9 (10.0–12.0)	10.2 (8.5–11.6)
Glucose tolerance, total AUC	1,484 (1,400–1,603)	1,397 (1,289–1,488)	1,915 (1,826–2,066)	1,649 (1,508–1,743)
Fasting insulin, pg/mL	455.1 (275.8–719.2)	337.9 (250.6–582.4)	847.6 (600.8–970.9)	747.2 (538.2–1,190.0)
Liver triglycerides, μmol glycerol/mg	14.88 (12.05–18.29)	12.85 (10.55–16.96)	23.83 (15.47–50.42)	18.10 (16.20–33.69)
Serum triglycerides, μg glycerol/mL	80.12 (66.76–93.47)	84.61 (70.99–123.2)	89.12 (66.85–96.77)	91.39 (79.92–124.5)
Serum HDL, mmol/L, *n* = 5–8	1.900 (1.775–1.995)	1.820 (1.595–1.890)	2.770 (2.480–2.900)	2.565 (2.108–2.695)
Serum cholesterol, mmol/L, *n* = 5–8	2.6 (2.5–2.8)	2.7 (1.9–2.8)	3.9 (3.8–4.2)	3.8 (3.3–4.0)
Serum glycerol, ng/mL	74.89 (63.2–84.68)	67.94 (56.09–97.40)	72.72 (55.34–115.00)	84.62 (66.46–124.00)
WAT glucose clearance, ^{3}H-2-DOG dpm/g/min	2.77 (1.47–4.08)	2.49 (2.11–3.44)	2.16 (1.73–3.18)	3.69 (3.04–4.99)
Quadriceps ^{3}H-2-DOG clearance, ^{3}H-2-DOG dpm/g/min	13.11 (10.24–17.75)	18.13 (15.48–23.39)	13.41 (10.73–14.28)	14.34 (11.48–17.56)
Epididymal fat mass, mg	259 (248–354)	324 (299–375)	459 (308–600)	541 (431–605)
Retroperitoneal fat mass, mg	156 (132–181)	172 (141–184)	240 (156–368)	285 (230–313)
Interscapular brown fat mass, mg	79.4 (64.75–85.55)	74.8 (35–82.2)	72.4 (67.8–94.7)	85.3 (59.8–97.3)
Body weight, g	23.1 (22.6–24.1)	22.7 (22.0–24.8)	23.2 (22.0–25.1)	23.3 (22.4–24.1)
Adipocyte diameter, μm^2	1,839 (1,708–1,852)	1,790 (1,700–1,867)	1,923 (1,814–2,009)	1,914 (1,891–1,992)
Glucose infusion rate (clamp), μmol/kg/min, *n* = 5–7	86.97 (43.05–94.69)	NA	9.89 (2.86–20.22)	51.46 (33.28–81.87)
Rate of disappearance (clamp), μmol/kg/min, *n* = 5–7	115.3 (84.38–135.8)	NA	71.63 (65.56–85.23)	87.65 (79.33–111.4)
Endogenous glucose production (clamp), μmol/kg/min, *n* = 5–7	41.19 (21.22–54.84)	NA	54.71 (52.47–83.16)	33.29 (29.5–47.5)

See Figs. 2 and 7. Values shown are median (interquartile range) and represent 14–19 animals per group unless otherwise indicated. NA, not applicable.

mice (Supplementary Table 1). No change was observed, indicating that the cytokines measured do not play a role in mediating metabolic changes with VEGF neutralization.

We next measured the effect of VEGF neutralization on adipocyte diameter, fat depot size, and whole-body adiposity, as changes in these parameters have also been implicated in changes to whole-body insulin sensitivity. There was a pronounced increase in the size of epididymal and inguinal fat pads, as well as adipocyte diameter, in control animals after 3 days of HFD, which was not affected by VEGF-A neutralization (Fig. 6*A* and *F*, Table 1). We next measured whole-body adiposity by dual-energy X-ray absorptiometry scanning and again observed an increase in adiposity with high-fat feeding, with no reduction following VEGF neutralization (Fig. 6*B*). Using a long-term model of high-fat feeding (Fig. 3), we also observed no change in epididymal fat pad mass or whole-body adiposity determined by dual-energy X-ray absorptiometry in animals treated with the VEGF antibody (Fig. 6*C* and *D*). In contrast to previous studies (20–22), these data suggest that improvements in insulin sensitivity and glucose tolerance occur independently of changes in adiposity and are consistent with a previous report showing no change in adiposity with systemic antibody neutralization of VEGF-R2 (38).

Evidence for Altered Lipid Uptake With VEGF Neutralization

We next quantified the level of triglyceride in liver and muscle tissues since previous studies have shown that antiangiogenic compounds reduce ectopic lipid deposition. As expected, high-fat feeding increased triglyceride content in both liver (Fig. 7*A*) and muscle (Fig. 7*B*); however, this was reduced by VEGF neutralization in muscle only. Intriguingly, VEGF neutralization raised serum triglyceride levels under both chow and high-fat conditions (Fig. 7*C*) while there was no change in circulating free glycerol levels (Fig. 7*D*). These data support the idea that muscle triglyceride levels are reduced with VEGF neutralization due to decreased lipid uptake, rather than increased β oxidation, which would have decreased serum triglycerides and increased free glycerol in the blood. One possibility for the increase in serum triglycerides is decreased uptake of lipid particles from the bloodstream into the liver, which occurs via fenestrations in the hepatic sinusoid, whose formation is VEGF dependent (39). We performed scanning electron microscopy of hepatic sinusoidal endothelial cells (Supplementary Fig. 5) and observed no trend in fenestration frequency, diameter, or porosity, suggesting some other mechanism is at play.

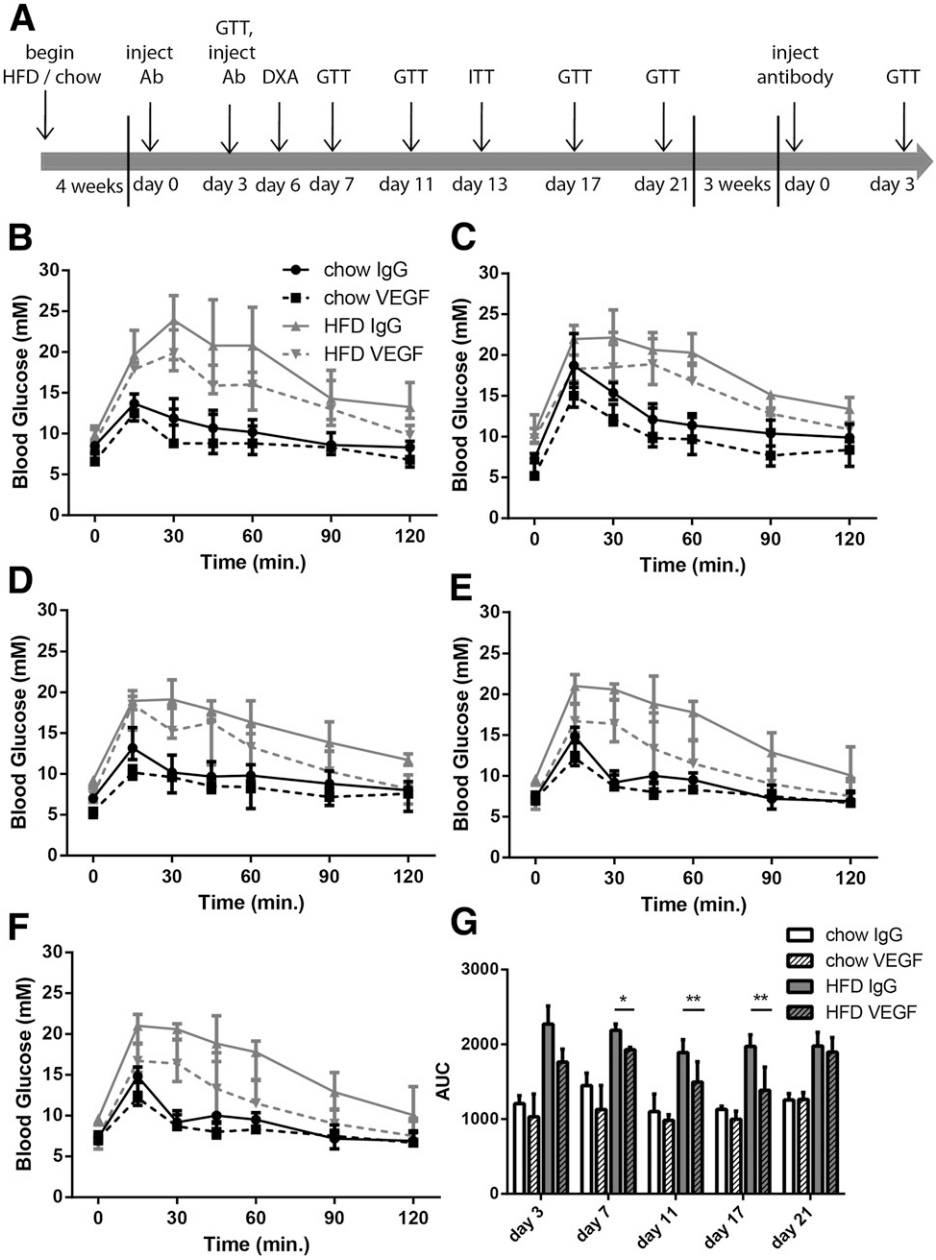

Figure 3—VEGF neutralization in long-term high-fat–fed mice. *A*: Eight-week-old mice were placed on chow diet or HFD for 4 weeks and were administered a single injection of either VEGF-neutralizing or control antibody at days 0 and 3. Glucose tolerance was assessed (*B*) 3 days after the first single injection and again at (*C*) day 7, (*D*) day 11, (*E*) day 17, and (*F*) day 21. *G*: Glucose tolerance was quantified by measuring AUCs. $n = 5–8$ mice per group. $^{*}P < 0.05$; $^{**}P < 0.01$, Kruskal–Wallis test. Glucose levels are plotted as median values, and error bars are interquartile range. Ab, antibody; DXA, dual-energy X-ray absorptiometry; ITT, insulin tolerance test.

DISCUSSION

In the current study, we have shown that systemic VEGF neutralization is a rapid and effective strategy for improving glucose tolerance and insulin sensitivity under both chow and high-fat conditions. VEGF neutralization not only prevented glucose intolerance upon induction of high-fat feeding, but reversed glucose intolerance in long-term high-fat fed mice. These improvements persisted for 17 days after administration of the VEGF-neutralizing antibody, though they were ameliorated by 21 days. The rapid, and eventually reversible, nature suggests that these effects are mediated through a persistent, ongoing maintenance process, such as vascular remodeling. The vasculature of adipose tissue was previously identified as a target for reducing obesity and improving metabolic homeostasis (20–22,24,25), yet we observed no change in adipocyte diameter, fat pad mass, or overall adiposity (Fig. 6). VEGF neutralization resulted in profound amelioration of hepatic insulin resistance following 3 days of high-fat feeding (Fig. 5).

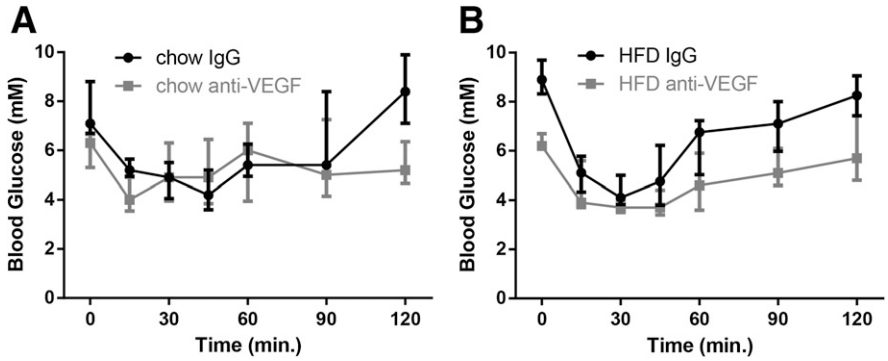

Figure 4—Insulin tolerance during VEGF neutralization in (*A*) chow and (*B*) long-term high-fat–fed mice. Long-term high-fat–fed animals were injected with VEGF-neutralizing antibody (5 mg/kg) at day 0 and day 3 as shown in Fig. 2*A*. At day 13, animals were subjected to insulin tolerance test (0.75 units/kg). n = 5–8 mice per group. Values shown are median, and error bars are interquartile range.

These effects of VEGF neutralization on the liver are in agreement with two recent studies (40,41). The lack of effect in peripheral glucose disposal further highlights the importance of the liver.

Interestingly, we observed increased serum triglycerides (Fig. 7*C*) with VEGF-A antibody treatment. This increase in serum triglycerides may not reflect a change in angiogenesis per se, but rather an alternate action of VEGF-A. For example, VEGF-B, another VEGF family member with partial homology to VEGF-A, regulates lipid uptake across the endothelium into tissues (4). Recently, it was shown that genetic ablation or antibody neutralization of VEGF-B protected against metabolic dysfunction in diet or genetic models of insulin resistance (5), due to reduced ectopic lipid deposition into muscle (5). It is possible that VEGF-A has similar effects to VEGF-B in blocking lipid uptake into tissues, which might explain increased serum triglycerides and decreased ectopic lipid deposition into muscle of chow-fed mice. Consistent with this hypothesis, in a recent study from Sun et al. (13), antibody neutralization of VEGF impaired lipid uptake into tissues of high-fat–fed mice, as measured by a lipid tolerance test.

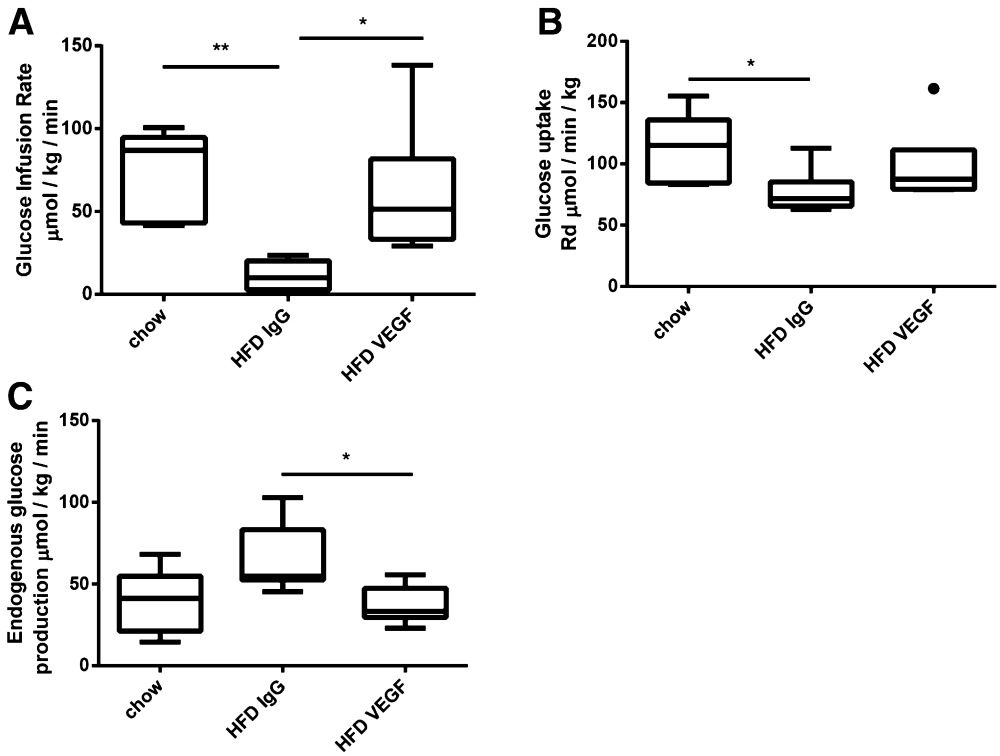

Figure 5—Insulin sensitivity and hepatic glucose output during VEGF neutralization. Hyperinsulinemic–euglycemic clamps were performed 72 h after treatment with VEGF-neutralizing or control antibody and chow or high-fat feeding as in Fig. 1. (*A*) Glucose infusion rate, (*B*) rate of disappearance, and (*C*) endogenous glucose output from the liver. n = 5–7 mice per group. *$P < 0.05$; **$P < 0.01$ Kruskal–Wallis test. Large dots are outliers, as per representation of data using Tukey box plot format. Rd, rate of disappearance.

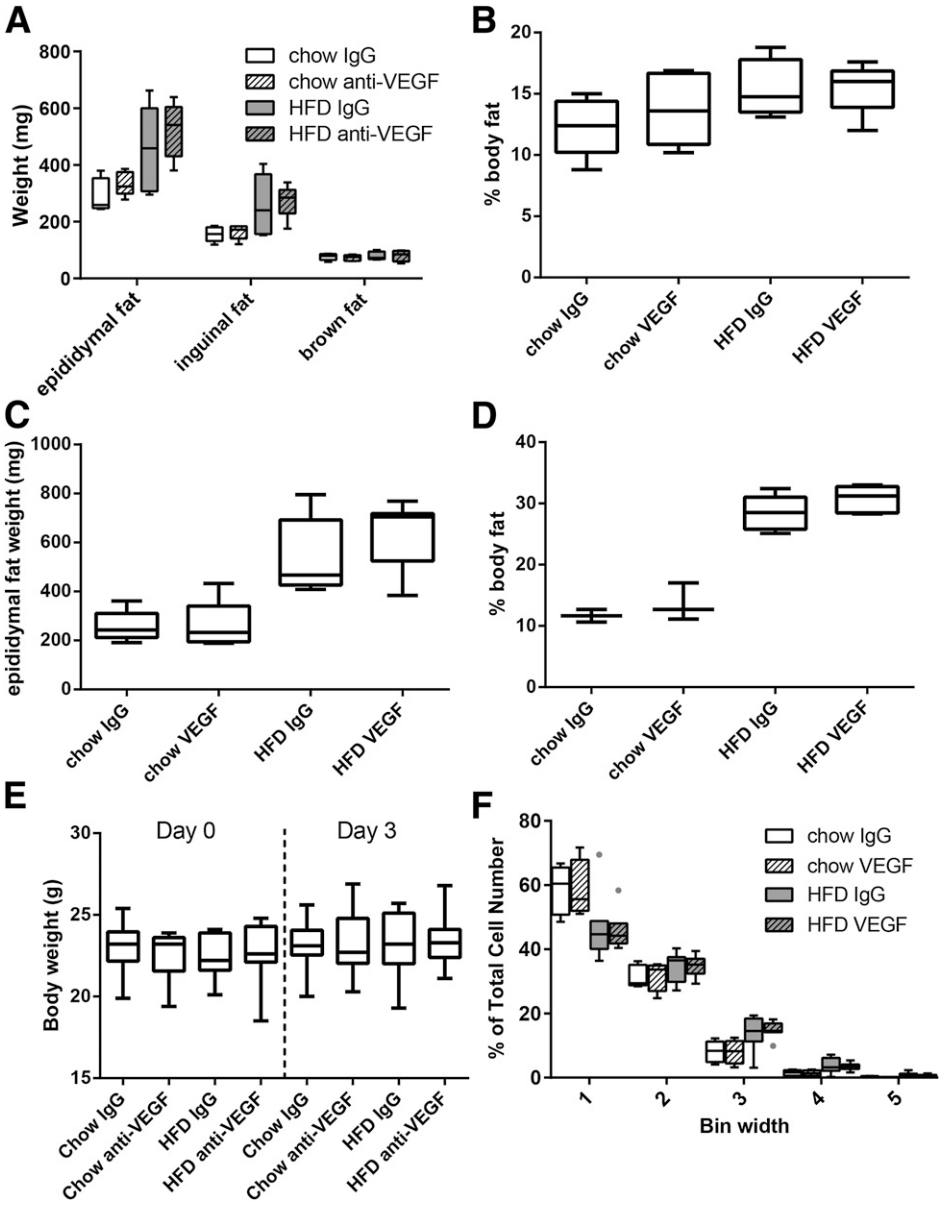

Figure 6—Adiposity during VEGF neutralization. (*A*) Fat pad mass and (*B*) percentage whole-body fat in an acute model of high-fat feeding and VEGF neutralization (Fig. 1); n = 14–19 mice per group. (*C*) Epididymal fat pad mass and (*D*) whole-body fat during a long-term model of high-fat feeding (Fig. 2); n = 5–8 mice per group. *E*: Body weights before and after acute high-fat feeding and VEGF treatment. *F*: Frequency distribution of adipocyte size in the 3-day model of VEGF treatment. Large dots are outliers, as per representation of data using Tukey box plot format.

It has been shown that VEGF positively regulates metabolic homeostasis. These findings were based on adipocyte-specific overexpression or deletion of VEGF (13–15) and so may reflect a long-term local effect of VEGF in adipose tissue. Conversely, systemic modulation of VEGF function as used here and in other studies (40,41) that describe positive effects of neutralizing VEGF function likely reflect effects of VEGF in alternate tissues, such as the liver. However, we also observed positive effects of neutralizing VEGF on insulin action in adipose tissue (Fig. 2). This leaves open the possibility that genetic manipulation of VEGF in adipose tissue gives rise to some chronic change in adipose function, possibly even developmental, which is not observed with the shorter-term systemic administration of VEGF-neutralizing antibody.

We examined insulin signaling at the level of Akt to determine whether improvements in glucose transport in WAT could be attributed to enhanced signal transduction. There was no change in Akt phosphorylation following VEGF neutralization. Although Akt activation is both necessary and sufficient to transduce the insulin signal to enhance glucose transport in adipocytes (42), we cannot rule out the involvement of alternate signaling pathways, such as atypical protein kinase C (43). Insulin suppresses lipolysis in WAT via both Akt-dependent and Akt-independent signaling pathways through HSL or perilipin, respectively (44). We did

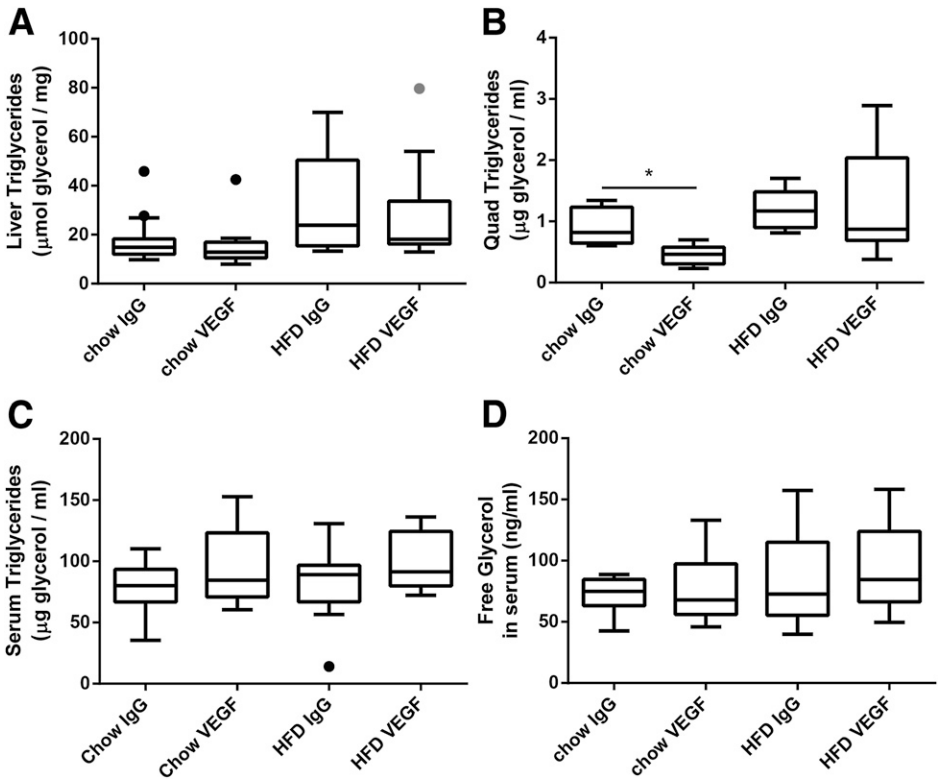

Figure 7—Ectopic lipids in VEGF antibody–treated mice. Triglyceride content in (*A*) liver, (*B*) quadriceps (*$P < 0.05$, Mann–Whitney test), (*C*) serum ($P < 0.05$, antibody effect, two-way ANOVA), and (*D*) free glycerol content in serum in mice 72 h after administration of VEGF-neutralizing antibody and high-fat feeding as described in Figs. 1 and 4. n = 14–19 mice per group. Large dots are outliers, as per representation of data using Tukey box plot format. Quad, quadriceps.

not detect changes in HSL or perilipin phosphorylation (Supplementary Fig. 4). These data suggest that both Akt-dependent and Akt-independent pathways, at least in the case of lipolysis, are not influenced by VEGF neutralization.

One key question regarding these findings is how VEGF neutralization so rapidly modulates insulin sensitivity in the liver. It is conceivable that this observation has significant bearing on the mechanism by which dietary manipulations such as HFD rapidly induce insulin resistance in the liver (36). Vascular remodeling in the liver following VEGF neutralization has been reported to activate the hypoxia-inducible factor-2α pathway, induce insulin receptor substrate (IRS) 2 expression and improve insulin signaling (40,41). In contrast, we did not observe any detectable change in downstream Akt signaling following VEGF neutralization (Supplementary Fig. 4). We have previously shown that defects in IRS signaling are unlikely to contribute to insulin resistance (27). Unlike the partial restoration of IRS2 observed in these recent studies (40,41), complete genetic deletion of IRS2 in the liver has no measurable effect on hepatic glucose homeostasis (45). Given this, there is no plausible explanation as to why an increase in IRS2 levels would be sufficient to improve insulin action in the absence of other changes. We therefore believe that some other mechanism most likely accounts for the effects of VEGF on liver metabolism. It is notable that microvascular blood flow is impaired in the liver of obese rodents due to a combination of ballooning of hepatocytes, distorting hepatic sinusoidal endothelial cells, collagen deposition in the spaces of Disse, and recruitment of proinflammatory, nonparenchymal cell types to the microvasculature, which could impair blood flow (46). VEGF is a potent vasodilator, and it is likely that VEGF neutralization would further impair vasodilation, which is required for insulin sensitivity. Changes in vasodilation are therefore unlikely to account for the improved insulin sensitivity observed during VEGF neutralization.

In conclusion, we have shown that VEGF neutralization results in a rapid and sustained improvement in overall glucose homeostasis, an effect primarily mediated by changes in hepatic insulin sensitivity. In view of the untoward side effects associated with systemic manipulation of VEGF action, it is unlikely that this will provide a practical therapeutic approach for the management of insulin resistance. It is therefore essential to pinpoint the mode of action of VEGF neutralization in the liver that so effectively reverses insulin resistance in HFD mice.

Acknowledgments. The authors thank members of the Diabetes and Obesity Program at the Garvan Institute and the Department of Pharmacology at University of New South Wales for help with discussions regarding this work.

Funding. L.E.W. is supported by an Early Career Fellowship from Cancer Institute New South Wales, Australia. This work was supported by a program grant from the NHMRC of Australia. D.E.J. is a senior principal research fellow of the NHMRC.

Duality of Interest. G.K. and N.v.B. are paid employees of Genentech, which holds a commercial interest in VEGF inhibitors, including the VEGF-neutralizing antibody B-20.4.1 used in this study. No other potential conflicts of interest relevant to this article were reported.

Author Contributions. L.E.W. conceived study, designed and performed experiments, analyzed data, and wrote the manuscript. C.C.M. designed and performed experiments, analyzed data, and provided input into the manuscript. S.P.M., D.J.F., V.C.C., M.M., H.P., M.-J.K., E.P., J.G.B., C.E.X., and G.K. performed experiments and provided critical input. A.S.M., J.S., N.v.B., J.R.G., D.G.L.C., G.J.C., and S.A. provided critical input into data interpretation. D.E.J. conceived study, interpreted data, and provided input into the manuscript. L.E.W. is the guarantor of this work and, as such, had full access to all the data in the study and takes responsibility for the integrity of the data and the accuracy of the data analysis.

References

1. Segerström L, Fuchs D, Bäckman U, Holmquist K, Christofferson R, Azarbayjani F. The anti-VEGF antibody bevacizumab potently reduces the growth rate of high-risk neuroblastoma xenografts. Pediatr Res 2006;60:576–581
2. Claes F, Vandevelde W, Moons L, Tjwa M. Another angiogenesis-independent role for VEGF: SDF1-dependent cardiac repair via cardiac stem cells. Cardiovasc Res 2011;91:369–370
3. Tjwa M, Luttun A, Autiero M, Carmeliet P. VEGF and PlGF: two pleiotropic growth factors with distinct roles in development and homeostasis. Cell Tissue Res 2003;314:5–14
4. Hagberg CE, Falkevall A, Wang X, et al. Vascular endothelial growth factor B controls endothelial fatty acid uptake. Nature 2010;464:917–921
5. Hagberg CE, Mehlem A, Falkevall A, et al. Targeting VEGF-B as a novel treatment for insulin resistance and type 2 diabetes. Nature 2012;490:426–430
6. Lu X, Zheng Y. Comment on: Elias et al. Adipose tissue overexpression of vascular endothelial growth factor protects against diet-induced obesity and insulin resistance. Diabetes 2012;61:1801-1813. Diabetes 2013;62:e3
7. Elias I, Franckhauser S, Bosch F. Response to Comment on: Elias et al. Adipose tissue overexpression of vascular endothelial growth factor protects against diet-induced obesity and insulin resistance. Diabetes 2012;61:1801-1813. Diabetes 2013;62:e4
8. Yilmaz M, Hotamisligil GS. Damned if you do, damned if you don't: the conundrum of adipose tissue vascularization. Cell Metab 2013;17:7–9
9. Loebig M, Klement J, Schmoller A, et al. Evidence for a relationship between VEGF and BMI independent of insulin sensitivity by glucose clamp procedure in a homogenous group healthy young men. PLoS ONE 2010;5:e12610
10. García de la Torre N, Rubio MA, Bordiú E, et al. Effects of weight loss after bariatric surgery for morbid obesity on vascular endothelial growth factor-A, adipocytokines, and insulin. J Clin Endocrinol Metab 2008;93:4276–4281
11. Silha JV, Krsek M, Sucharda P, Murphy LJ. Angiogenic factors are elevated in overweight and obese individuals. Int J Obes (Lond) 2005;29:1308–1314
12. Lu X, Ji Y, Zhang L, et al. Resistance to obesity by repression of VEGF gene expression through induction of brown-like adipocyte differentiation. Endocrinology 2012;153:3123–3132
13. Sun K, Wernstedt Asterholm I, Kusminski CM, et al. Dichotomous effects of VEGF-A on adipose tissue dysfunction. Proc Natl Acad Sci U S A 2012;109:5874–5879
14. Sung HK, Doh KO, Son JE, et al. Adipose vascular endothelial growth factor regulates metabolic homeostasis through angiogenesis. Cell Metab 2013;17:61–72
15. Elias I, Franckhauser S, Ferré T, et al. Adipose tissue overexpression of vascular endothelial growth factor protects against diet-induced obesity and insulin resistance. Diabetes 2012;61:1801–1813
16. Mullican SE, Tomaru T, Gaddis CA, Peed LC, Sundaram A, Lazar MA. A novel adipose-specific gene deletion model demonstrates potential pitfalls of existing methods. Mol Endocrinol 2013;27:127–134
17. Elmasri H, Karaaslan C, Teper Y, et al. Fatty acid binding protein 4 is a target of VEGF and a regulator of cell proliferation in endothelial cells. FASEB J 2009;23:3865–3873
18. Gerber HP, Malik AK, Solar GP, et al. VEGF regulates haematopoietic stem cell survival by an internal autocrine loop mechanism. Nature 2002;417:954–958
19. Lee S, Chen TT, Barber CL, et al. Autocrine VEGF signaling is required for vascular homeostasis. Cell 2007;130:691–703
20. Bråkenhielm E, Cao R, Gao B, et al. Angiogenesis inhibitor, TNP-470, prevents diet-induced and genetic obesity in mice. Circ Res 2004;94:1579–1588
21. Kolonin MG, Saha PK, Chan L, Pasqualini R, Arap W. Reversal of obesity by targeted ablation of adipose tissue. Nat Med 2004;10:625–632
22. Rupnick MA, Panigrahy D, Zhang CY, et al. Adipose tissue mass can be regulated through the vasculature. Proc Natl Acad Sci U S A 2002;99:10730–10735
23. Liang WC, Wu X, Peale FV, et al. Cross-species vascular endothelial growth factor (VEGF)-blocking antibodies completely inhibit the growth of human tumor xenografts and measure the contribution of stromal VEGF. J Biol Chem 2006;281:951–961
24. Cao Y. Adipose tissue angiogenesis as a therapeutic target for obesity and metabolic diseases. Nat Rev Drug Discov 2010;9:107–115
25. Cao Y. Angiogenesis modulates adipogenesis and obesity. J Clin Invest 2007;117:2362–2368
26. Bruce CR, Hoy AJ, Turner N, et al. Overexpression of carnitine palmitoyltransferase-1 in skeletal muscle is sufficient to enhance fatty acid oxidation and improve high-fat diet-induced insulin resistance. Diabetes 2009;58:550–558
27. Hoehn KL, Hohnen-Behrens C, Cederberg A, et al. IRS1-independent defects define major nodes of insulin resistance. Cell Metab 2008;7:421–433
28. Hoehn KL, Salmon AB, Hohnen-Behrens C, et al. Insulin resistance is a cellular antioxidant defense mechanism. Proc Natl Acad Sci U S A 2009;106:17787–17792
29. Hoehn KL, Turner N, Swarbrick MM, et al. Acute or chronic upregulation of mitochondrial fatty acid oxidation has no net effect on whole-body energy expenditure or adiposity. Cell Metab 2010;11:70–76
30. Mangiafico SP, Lim SH, Neoh S, et al. A primary defect in glucose production alone cannot induce glucose intolerance without defects in insulin secretion. J Endocrinol 2011;210:335–347
31. Cogger VC, Svistounov D, Warren A, et al. Liver Aging and Pseudocapillarization in a Werner Syndrome Mouse Model. J Gerontol A Biol Sci Med Sci. 22 Oct 2013 [Epub ahead of print]
32. Fuh G, Wu P, Liang WC, et al. Structure-function studies of two synthetic anti-vascular endothelial growth factor Fabs and comparison with the Avastin Fab. J Biol Chem 2006;281:6625–6631
33. Yang JC, Haworth L, Sherry RM, et al. A randomized trial of bevacizumab, an anti-vascular endothelial growth factor antibody, for metastatic renal cancer. N Engl J Med 2003;349:427–434
34. Willett CG, Boucher Y, Duda DG, et al. Surrogate markers for antiangiogenic therapy and dose-limiting toxicities for bevacizumab with radiation and chemotherapy: continued experience of a phase I trial in rectal cancer patients. J Clin Oncol 2005;23:8136–8139
35. Finley SD, Engel-Stefanini MO, Imoukhuede PI, Popel AS. Pharmacokinetics and pharmacodynamics of VEGF-neutralizing antibodies. BMC Syst Biol 2011;5:193
36. Turner N, Kowalski GM, Leslie SJ, et al. Distinct patterns of tissue-specific lipid accumulation during the induction of insulin resistance in mice by high-fat feeding. Diabetologia 2013;56:1638–1648

37. Kraegen EW, Clark PW, Jenkins AB, Daley EA, Chisholm DJ, Storlien LH. Development of muscle insulin resistance after liver insulin resistance in high-fat-fed rats. Diabetes 1991;40:1397–1403
38. Lijnen HR, Scroyen I. Effect of vascular endothelial growth factor receptor 2 antagonism on adiposity in obese mice. J Mol Endocrinol 2013;50:319–324
39. Carpenter B, Lin Y, Stoll S, Raffai RL, McCuskey R, Wang R. VEGF is crucial for the hepatic vascular development required for lipoprotein uptake. Development 2005;132:3293–3303
40. Taniguchi CM, Finger EC, Krieg AJ, et al. Cross-talk between hypoxia and insulin signaling through Phd3 regulates hepatic glucose and lipid metabolism and ameliorates diabetes. Nat Med 2013;19:1325–1330
41. Wei K, Piecewicz SM, McGinnis LM, et al. A liver Hif-2α-Irs2 pathway sensitizes hepatic insulin signaling and is modulated by Vegf inhibition. Nat Med 2013;19:1331–1337
42. Ng Y, Ramm G, Lopez JA, James DE. Rapid activation of Akt2 is sufficient to stimulate GLUT4 translocation in 3T3-L1 adipocytes. Cell Metab 2008;7:348–356
43. Standaert ML, Galloway L, Karnam P, Bandyopadhyay G, Moscat J, Farese RV. Protein kinase C-zeta as a downstream effector of phosphatidylinositol 3-kinase during insulin stimulation in rat adipocytes. Potential role in glucose transport. J Biol Chem 1997;272:30075–30082
44. Choi SM, Tucker DF, Gross DN, et al. Insulin regulates adipocyte lipolysis via an Akt-independent signaling pathway. Mol Cell Biol 2010;30:5009–5020
45. Simmgen M, Knauf C, Lopez M, et al. Liver-specific deletion of insulin receptor substrate 2 does not impair hepatic glucose and lipid metabolism in mice. Diabetologia 2006;49:552–561
46. Farrell GC, Teoh NC, McCuskey RS. Hepatic microcirculation in fatty liver disease. Anat Rec (Hoboken) 2008;291:684–692